Observation of Interference in Charge Exchange Scattering in $He^{2+} + He^{+}$ Collisions

S. Krüdener, F. Melchert, K. v. Diemar, A. Pfeiffer, K. Huber, and E. Salzborn
Institut für Kernphysik, Universität Giessen, 35392 Giessen, Germany

D. B. Uskov and L. P. Presnyakov
P. N. Lebedev Physical Institute, 117924 Moscow, Russia
(Received 15 May 1997)

We report the first observation of interference in charge exchange collisions between two ions. Employing the crossed-beams technique in conjunction with signal recovery methods, angular differential cross sections have been measured for charge transfer in $He^{2+} + He^{+}$ collisions at barycentric energies between 0.5 and 10.2 keV. The oscillatory structure observed is in agreement with quantum calculations and can be interpreted in terms of interference between scattering into *gerade* and *ungerade* molecular states, which arise due to the identity of the nuclear charges. [S0031-9007(97)03776-9]

PACS numbers: 34.70.+e, 52.20.Hv

In this Letter, we report on the first measurements of angular differential cross sections for charge transfer between a bare and a singly-charged He ion:

$$He^{2+} + He^{+}(1s) \rightarrow He^{+}(1s) + He^{2+}. \quad (1)$$

This reaction exhibits unique features since it represents a one-electron, charge-symmetric collision system resonant for $1s \rightarrow 1s$ electron transfer.

In contrast to ion-*atom* collisions, where electron capture processes have been studied in great detail over many decades, experimentally as well as theoretically, in ion-*ion* collisions there prevails Coulomb repulsion both in the incoming and outgoing reaction channel. Therefore, the collision system studied provides an ideal testing ground for the study of the effect of long-range Coulomb interaction in the quantum three-body problem.

The results obtained show that it is virtually impossible to predict the differential cross section of reaction (1) by scaling the pioneering data available from the past thirty years for the isoelectronic ion-atom collision system $H^{+} + H$ [1–5].

In this paper we also present quantum calculations based on a partial wave analysis using a molecular basis and taking into account rotational coupling. These calculations are in good agreement with the experimental data whereas the comparison with a semiclassical calculation [6] shows some discrepancies. The oscillations observed in the differential cross section for scattering angles ranging from 0° to approximately 5° are due to interference between *gerade* and *ungerade* molecular states. These interferences between different molecular states have first been observed in the pioneering experiments of the collisions of H^{+} or He^{+} projectiles with H or He gas targets [1,7,8]. This effect also occurs in *K*-*K* shell vacancy transfer in collisions between highly charged ions and atoms [9,10]. The oscillations cannot result from *rainbow scattering* since there is no attractive potential due to the Coulomb repulsion in all channels.

For the experiment we have employed the crossed-beams technique in conjunction with coincident detection of both reaction products. However, in order to measure the scattering distributions of the He^{+} reaction products, we had to upgrade essential features of the Giessen ion-ion crossed-beams facility described previously [11]. First, the entire ion-optical beam preparation and analysis system was replaced to change the intersection angle between the two ion beams from 45° (used previously) to 17.5° (used now). This gives access to lower collision energies. Second, we optimized the beam transport system to provide intense ion beams of high brightness. Third, we installed a position sensitive detector (diameter 4 cm) and applied list mode techniques for data acquisition. This new setup is described in full detail in Ref. [12].

The He ion beams collide in an ultrahigh vacuum of less than 10^{-10} mbar. The main difficulties stem from low signal rates of a few events per sec. This low signal rate is distributed over a position matrix of typically 100×100 channels. This leads to an average count rate of about 10^{-4}–10^{-3} events per channel per sec, which is masked by up to 4 orders of magnitude higher background rates due to ion-residual gas reactions of the 10^{12} times more intense primary beam. For signal recovery, we make use of the coincident detection of both reaction products.

Extraction of differential cross sections from measured scattering distributions requires the transformation between lab- and c.m.-system as well as appropriate knowledge of the primary ion beam profile. The c.m.-lab transformation does not conserve rotational symmetry due to the crossed-beams kinematics. The primary ion beam profile (beam radius $r \approx 0.8$ mm, divergence half angle $\Delta\alpha \approx 0.1°$) broadens the observed scattering distribution and smears out structures. In order to compare results obtained experimentally with theoretical calculations the experimental data can be deconvoluted with respect to the primary ion beam profile or theoretically calculated differential cross sections can be convoluted with the

 0031-9007/97/79(6)/1002(4)$10.00

corresponding primary ion beam profile. For the deconvolution procedure, often Fourier-transformation methods are applied. These methods have been successful when noise content in the degraded signal distribution is moderate or small. However, at increased noise or decreased signal levels Fourier methods have failed to produce reliable deconvoluted data [13]. Therefore an iterative self-correcting deconvolution technique based on Bayesian deconvolution [13] was applied to this problem. The idea of this method is to vary a reasonable start distribution for the deconvoluted result until the convolution of this data yields the original measurement. We used smoothed experimental data as start distributions.

We measured the ion beam profile in one dimension on an absolute scale by moving a horizontal slit at the interaction point across the collision plane. In two dimensions we measured He^+ ions produced only in fast (e.g., $E_{\mathrm{lab}} = 15$ keV) He^{2+}-residual gas collisions by detuning the time coincidence window. In contrast to ion-ion reactions, where Coulomb repulsion at low c.m. energies (e.g., $E_{\mathrm{c.m.}} = 2.5$ keV or less) plays an important role, fast ion-residual gas collision products are scattered only by small polar angles θ, independent of the azimuthal angle φ. Assessment of the absolute ion beam profile is achieved by combining the absolute information in one dimension and the relative information in two dimensions.

Figure 1(a) shows a smoothed scattering distribution measured at $E_{\mathrm{c.m.}} = 2.5$ keV. The apparent structures are smeared out by the primary ion beam profile. The deconvoluted result [Fig. 1(b)] is obtained after 100 iterations. The z axis of both plots is drawn on a natural logarithmic scale. The minimum in the forward direction is surrounded by symmetric structures with rapidly decreasing amplitudes. For large scattering angles numerical fluctuations due to very low signal rates are introduced by the deconvolution algorithm. After integration over the azimuthal angle φ when extracting angular differential cross sections from Fig. 1(b), the influence of these fluctuations on the angular differential cross section is reduced. The scattering distribution shown in Fig. 1(a) contains about 1 million events collected in 24 h. Typical ion currents of 1.2 nA for the He^{2+} and 13 μA for the He^+ ion beam lead to a count rate of about 10 events per sec. The total cross section was normalized to our previous measurements [11] as 5.2×10^{-16} cm^2. Figure 2(a) shows the angular differential cross section $d\sigma/d\Omega$ obtained by integration of the data in Fig. 1(b) over the azimuthal angle φ as a function of the c.m.-scattering angle $\theta_{\mathrm{c.m.}}$. The deconvoluted data for c.m.-scattering angles up to 3.2° show an oscillatory structure including four maxima. In addition to the minimum in forward direction, another four minima are resolved experimentally. The oscillation period increases with scattering angles. Figure 2(a) also compares the present experimental data with both the semiclassical eikonal calculation [6] (dotted line) and the present quantum calculation (solid line) described below. In the semiclassical impact parameter method [6] the electronic wave

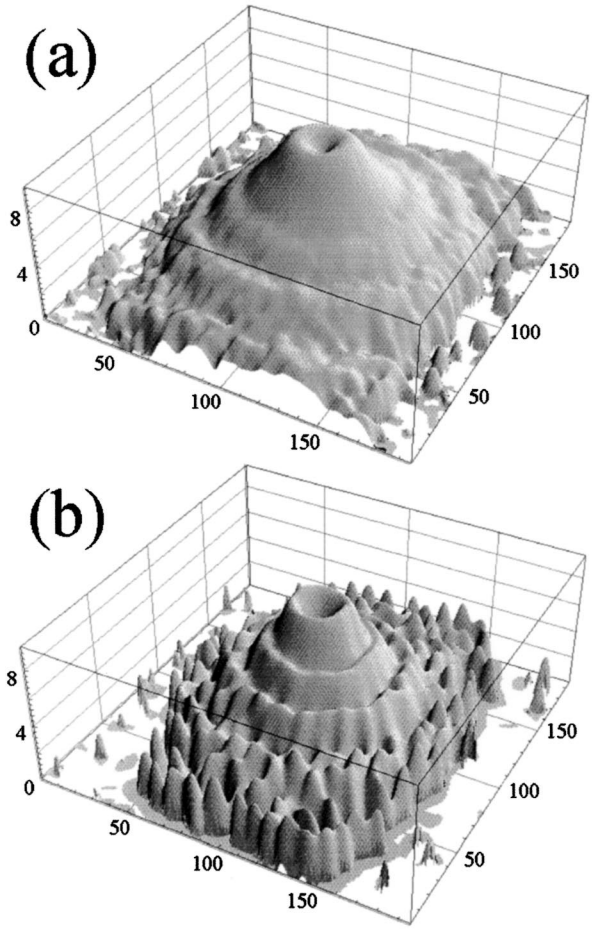

FIG. 1. Three-dimensional view of the scattering distribution of He^+ ions produced in He^{2+}-He^+ collisions at $E_{\mathrm{c.m.}} = 2.5$ keV, drawn on a natural logarithmic z scale. Channel numbers on x and y axes equal 0.156 mm/channel, i.e., 0.00815°/channel. (a) Smoothed raw data; (b) deconvoluted data.

functions are expanded in terms of atomic orbitals. Taking into account Coulomb trajectories a two-state expansion was used employing the eikonal approximation. For small scattering angles $\theta_{\mathrm{c.m.}}$ up to the second maximum there is fair agreement between experiment and the semiclassical calculation. For larger scattering angles, however, this theoretical approach [6] shows a longer period for the following structures, resulting in a kind of "phase shift" between the experimental and theoretical curve.

The remarkable oscillatory structures in the differential charge-transfer cross sections can be interpreted as interference between *gerade* and *ungerade* electronic states of the ionic molecule. This effect, predicted long ago [14,15], was widely discussed mainly on the basis of the impact parameter approach and was calculated for the isoelectronic H^+-H collision system using the three-state molecular expansion [4,5]. For reaction (1), we employed a quantum approach based on a partial wave analysis using a molecular basis. We also include the nonadiabatic rotational $2p\sigma_u$-$2p\pi_u$ coupling describing the capture into the excited $2p$ state and related scattering matrix-element corrections.

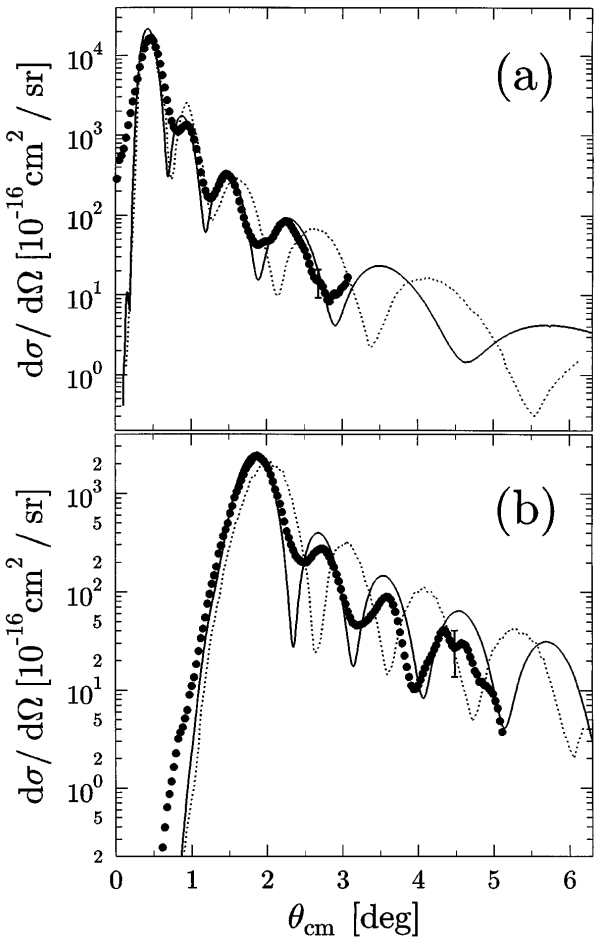

FIG. 2. Angular differential cross sections for the charge transfer process $He^{2+} + He^{+} \rightarrow He^{+} + He^{2+}$ at $E_{\mathrm{c.m.}} = 2.5$ keV (a) and $E_{\mathrm{c.m.}} = 0.5$ keV (b); •: experiment, solid line: present calculation, dotted line: semiclassical calculation [6].

Thus, the problem is reduced to solving the radial equations in the total angular momentum J representation (ignoring the electron spin), subject to the S-matrix boundary conditions. For the rotational coupling matrix element we use the Bates and Williams result [16] which accounts for the correct asymptotic properties of the rearrangement problem at infinity. The differential cross section for charge transfer to the $1s$ and $2p$ states is as follows:

$$\sigma(\theta) = \sigma_{1s}(\theta) + \sigma_{2p}(\theta), \tag{2}$$

$$\sigma_{1s}(\theta) = \left| \frac{1}{4ik} \sum_J (2J + 1) P_J(\cos\theta) \times (e^{i2\delta_0^J} - S_{11}^J e^{i2\delta_1^J}) \right|^2, \tag{3}$$

$$\sigma_{2p}(\theta) = \frac{k_2}{k} \left| \frac{1}{4ik} \sum_J (2J + 1) P_J(\cos\theta) S_{12}^J e^{i(\delta_1^J + \delta_2^J)} \right|^2. \tag{4}$$

Here δ_i^J are the phase shifts of pure elastic scattering in the uncoupled channels $i = 0, 1, 2$, corresponding to the $1s\sigma_g$, $2p\sigma_u$, and $2p\pi_u$ states, respectively; $k = k_0 = k_1$ and k_2 are the wave numbers of the relative motion. $S_{ii'}$ are the scattering matrix elements resulting from the rotational coupling between the channels 1 and 2.

The cross section for capture into the ground state (3) is expressed in terms of the Legendre polynomials because the electron orbital momentum in channel 0 and 1 is equal to 0. Capture into the excited $2p$ state (4) represents small corrections to σ_{1s}. The phase shifts δ_i^J were calculated with the help of an approach discussed earlier [17]. The sums of (3) and (4) were restricted to 7×10^3 terms. The nonadiabatic rotational coupling was found to be important for the positions of the cross section maxima and minima in the range of $\theta_{\mathrm{c.m.}} E_{\mathrm{c.m.}} > 5$ (deg keV). For smaller angles, the differential cross section is defined by interference of the $1s\sigma_g$ and $2p\sigma_u$ states only. For example, at the maximum collision energy of 2.5 keV, presented here, the additional phase due to the rotational coupling leads to the shift of the fifth maximum position by about 0.2° towards larger angles.

The quantum theory described above shows good agreement with the experimental data at $E_{\mathrm{c.m.}} = 2.5$ keV [Fig. 2(a)]. A phase shift for larger scattering angles is not observed here, in contrast to the semiclassical calculation (dotted line) which can be applied to scattering through small angles only as depicted in [6]. Figure 2(b) shows the angular differential cross section at $E_{\mathrm{c.m.}} = 0.5$ keV. There seems to be a structure within the fourth maximum around $\theta_{\mathrm{c.m.}} = 4.5°$. This cannot be interpreted as an additional pattern of oscillations arising from the nuclear symmetry due to the identical ^{4}He nuclei as has been observed by Aberth *et al.* [18] in $^4He^+ + {}^4$He ion-atom scattering at large scattering angles, since this structure is within the statistical error of the raw data, as indicated for one point, and since the influence of the indistinguishability of the ^{4}He nuclei is expected to be negligible for the range of small scattering angles depicted here. Comparing Figs. 2(a) and 2(b), the decreasing c.m. energy pronounces larger scattering angles $\theta_{\mathrm{c.m.}}$. Fair agreement exists between experiment and present calculation, while the semiclassical calculation [6] is running "out of phase."

Comparison between theory and experiment has also been studied on basis of the convolution of the theoretical calculations with the respective apparatus function: Again experimental data are in good agreement with present calculations whereas the atomic basis semiclassical eikonal approach [6] leads to deviations from experiment especially at larger scattering angles.

Besides the collision energies 0.5 and 2.5 keV discussed here in detail we have also measured angular differential cross sections for 14 additional energies between 0.62 and 10.2 keV. Maxima in the course of the angular differential cross section as a function of the c.m. energy are numbered $k = 1, \ldots, 5$ from small to large scattering angles. Figure 3 gives an overall view of the maxima's locations on a plot $E_{\mathrm{c.m.}}$ (maximum) vs $\theta_{\mathrm{c.m.}}$ (maximum). For most of the 14 additional measurements (open symbols) the statistics have not been sufficient for $k = 3$ and $k = 4$. In

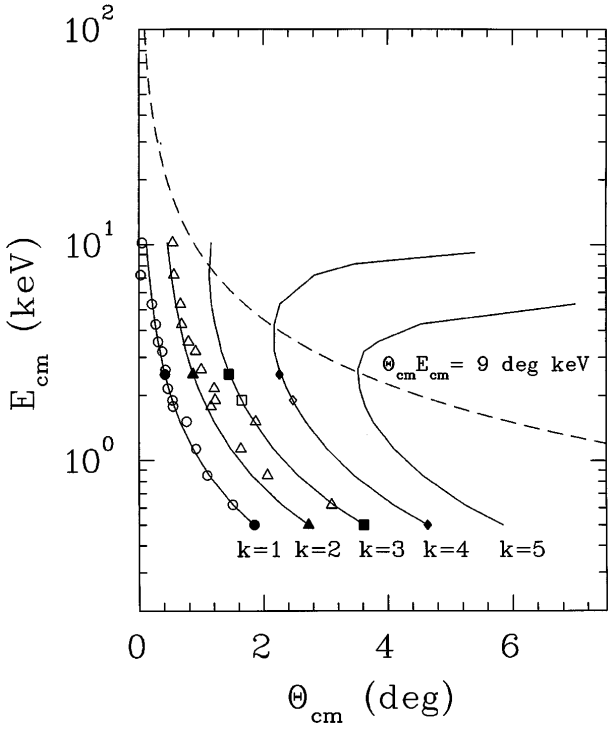

FIG. 3. Locations of the maxima in the angular differential cross section, plotted on $E_{\mathrm{c.m.}}$ (maximum) vs $\theta_{\mathrm{c.m.}}$ (maximum). Starting from zero degree scattering, maxima are numbered $k = 1, \ldots, 4$ with increasing scattering angle; circles: $k = 1$, triangles: $k = 2$, squares: $k = 3$, diamonds: $k = 4$, solid lines: present calculation; full symbols represent measurements with better statistics [see Figs. 2(a) and 2(b)].

addition, results of our quantum calculation are included in the plot as solid lines for $k = 1, \ldots, 5$. In the region where experimental data exist the location of maxima is shifting towards lower scattering angles with increasing energy, roughly satisfying $\theta_{\mathrm{c.m.}} = a_k/E_{\mathrm{c.m.}} + b_k$, where a_k and b_k are specific constants for each maximum k. Clearly seen for $k = 4$ and $k = 5$, the theoretical curve indicates that the maximum is smeared out over a wide angular range. A symmetry curve, shown as a broken line in Fig. 3, seems to appear around $\theta_{\mathrm{c.m.}}E_{\mathrm{c.m.}} \approx 9$ (deg keV) which means a constant impact parameter. This phenomenon is known for the isoelectronic $H^+ + H$ system [1] and also for the $He^+ + He$ system [7]. Nevertheless, there is a qualitative difference between those ion-atom systems and the ion-ion collision system (1) discussed here. In ion-ion collisions, the locations of maxima in the low energy range are shifted towards smaller scattering angles with increasing energy while this phenomenon is missing in ion-atom collision systems due to the lack of Coulomb repulsion at large internuclear distances. For ion-atom collision systems the locations of maxima are nearly independent of energy in the low energy region causing vertical lines in Fig. 3 for the different maxima at low energies, which is not valid in ion-ion collisions.

In summary, the present Letter is the first report on experimental angular differential cross sections in an ion-ion collision system. The results for the charge transfer process in $He^{2+} + He^+$ collisions are in fair agreement with the partial wave quantum calculation using a quasimolecular approach. In conclusion, we note that angular differential cross sections are more sensitive than total cross sections to the physical parameters of the process. For example, it is barely possible to establish a scaling law which could estimate the differential cross section in $He^{2+} + He^+$ collisions using the data available for $H^+ + H$ collisions. In ion-atom collisions, the internuclear potential shows an attractive outer region, while the inner region is repulsive. This leads to the oscillatory *rainbow scattering*, which is absent in ion-ion collisions.

This work was supported by Deutsche Forschungsgemeinschaft. The theoretical part was supported by an ISTC Grant for Project No. 076-95, INTAS Project No. 94-4698, and RFBR Project No. 96-02-16090-a. The authors appreciate fruitful discussions with Professor J. Briggs, Professor J. Burgdörfer, and Dr. W. Fritsch.

[1] H. F. Helbig and E. Everhart, Phys. Rev. **140**, A715 (1965).
[2] J. C. Houver, J. Fayeton, and M. Barat, J. Phys. B **7**, 1358 (1974).
[3] S. W. Knudsen and W. R. Thorsen, Can. J. Phys. **48**, 313 (1970).
[4] R. McCarroll and R. D. Piacentini, J. Phys. B **3**, 1336 (1970).
[5] C. Gaussorgues, C. LeSech, F. Masnou-Seeuws, R. McCarroll, and A. Riera, J. Phys. B **8**, 239 (1975); **8**, 253 (1975).
[6] C. Forster, R. Shingal, D. R. Flower, B. H. Bransden, and A. S. Dickinson, J. Phys. B **21**, 3941 (1988).
[7] C. Lockwood, H. Helbig, and E. Everhart, Phys. Rev. **132**, 2078 (1963).
[8] F. P. Ziemba, G. J. Lockwood, G. H. Morgan, and E. Everhart, Phys. Rev. **118**, 1552 (1960).
[9] R. Schuch, in *Proceedings of the XIV International Conference on the Physics of Electronic and Atomic Collisions, Palo Alto, 1985*, edited by D. C. Lorents, W. E. Meyerhof, and J. R. Peterson (North-Holland, Amsterdam, 1986).
[10] M. Schulz, E. Justiniano, J. Konrad, R. Schuch, and A. Salin, J. Phys. B **20**, 2057 (1987).
[11] F. Melchert, S. Krüdener, R. Schulze, S. Petri, S. Pfaff, and E. Salzborn, J. Phys. B **28**, L355 (1995).
[12] S. Meuser, F. Melchert, S. Krüdener, A. Pfeiffer, K. v. Diemar, and E. Salzborn, Rev. Sci. Instrum. **67**, 2752 (1996).
[13] W. H. Richardson, J. Opt. Soc. Am. **62**, 55 (1972).
[14] H. S. W. Massey and R. A. Smith, Proc. R. Soc. London A **142**, 142 (1933).
[15] O. B. Firsov, Zh. Eksp. Teor. Fiz. **21**, 1001 (1951).
[16] D. R. Bates and D. A. Williams, Proc. Phys. Soc. London **83**, 425 (1964).
[17] L. P. Presnyakov, Phys. Rev. A **44**, 5636 (1991).
[18] W. Aberth, D. C. Lorents, R. P. Marchi, and F. F. Smith, Phys. Rev. Lett. **14**, 776 (1965).